BER the international journal of bridge engineering management and research

Seismic Fragility and Risk Assessment of Reinforced Concrete Bridges Undergoing Elastomeric Bearing Deformations Induced by Landslide

Sergio Ruggieri[1]; Andrea Nettis[1]; Domenico Raffaele[1]; Biagio Guido[2]; and Giuseppina Uva[1,*]

Submitted: 09 January 2024 **Accepted:** 09 July 2024 **Publication date:** 03 September 2024

Abstract: The paper presents a study on the seismic fragility of Reinforced Concrete (RC) bridges isolated by elastomeric bearing devices subjected to differential displacements induced by slow-moving landslides. The seismic behavior of isolated bridges is ruled by the performance of elastomeric bearings to reduce and dissipate earthquake actions. These bridges are subjected to service loads that usually are accounted for in the design, but possible additional actions from the surrounding environment, such as landslides affecting substructure components, can seriously undermine the seismic response. The paper describes a practical approach to investigate the seismic fragility and risk of RC bridges isolated by elastomeric bearings, which may undergo early deformations induced by the differential displacements of substructure components. Based on previous existing studies, the proposed methodology is based on numerical modeling accounting for landslide-induced substructure displacements and proper modifications on the constitutive law and hysteretic response of the elastomeric bearings. Subsequently, after establishing specific limit-states, nonlinear time history analyses of the seismic response are used to estimate fragility curves and risk indicators. The study points out that it is possible to quantify the influence of landslide-induced effects on seismic fragility and risk by using only two numerical models in order to provide decision support to transportation authorities responsible for ensuring the safety of bridges and road networks. The proposed approach has been tested on a real-life case study, the *Santo Stefano* Viaduct in Italy, which was subjected in the past to relevant deformations of the elastomeric bearings due to an active landslide phenomenon.

Author keywords: Seismic fragility; existing RC bridges; elastomeric bearings; landslides, multi-hazard risk

Introduction

The study of the vulnerability of existing Reinforced Concrete (RC) bridges under natural and human-related hazards is one of the main challenges that the scientific community, public institutions, and road management companies are currently facing in light of recent tragic events that have been reported structural collapses and intangible financial and human losses, as well as the occurrence of extended downtime. For bridges and viaducts, the causes of collapse may be related to a combination of different hazardous sources, which should be considered together to correctly assess the structural health condition and prioritize retrofit interventions. Within this framework, several studies have been proposed in recent years by the scientific literature, with the aim of investigating multi-hazard risk sources affecting existing bridges (e.g., Gidaris et al.[1]). Seismic risk prioritization is one of the most studied topics in seismic hazard-prone areas. Starting from a view of the entire bridge stock in Italy, Borzi et al.[2] proposed an automatic tool to estimate the seismic fragility of bridges at two limit states (i.e., damage and collapse). The tool was tested on a sample of around 500 existing bridges for which good level information was available, and a WebGIS graphical user interface was released to observe real-time damage scenarios. Abarca et al.[3] investigated seismic risk and losses of more than 600 existing bridges in Southern Italy, creating a proper taxonomy on the basis of full complete structural information given by another bridge dataset and statistically investigating the seismic response of simulated archetypes. Obviously, large-scale studies based on typological approaches are possible when enough information is available. For portfolio-scale bridge assessment, single-structure simplified approaches can be mentioned, where the seismic fragility can be estimated through displacement-based assessment techniques characterized by different bridge typologies[4,5,6].

Current research trends are increasingly focusing on the vulnerability of bridges under geohazards and flood actions. Regarding geohazards, damages can be induced by differential settlements of the bridges related to soft soil strata (not properly considered in the design) or by low-moving ground movements affecting bridge foundations, typical of areas affected by active landslides. In these cases, for an appropriate risk assessment, monitoring campaigns

*Corresponding Author: Giuseppina Uva.
Email: giuseppina.uva@poliba.it
[1]DICATECH Department, Polytechnic University of Bari, Via Orabona 4, 70125, Bari, Italy
[2]ALEANDRI S.p.a, Corso Vittorio Emanuele II 52, 70122, Bari, Italy

should be provided, by employing specific instruments and long-time observations. Nevertheless, an important resource exploited in the last years is represented by multi-temporal satellite-based differential interferometry (MTInSAR) techniques, which allow to detect displacements of the terrestrial surface over a long range of time and assess the possible interference with existing bridges (or more in general with structures). Peduto et al.[7] proposed a framework based on MTInSAR data and on-site surveys to probabilistically assess the structural condition of existing bridges in Amsterdam and proposed fragility functions to describe current ground motion-induced damage conditions. Nettis et al.[8] developed an automated tool that elaborates the displacement histories of persistent scatters on bridges belonging to road networks and identifies the units subjected to geological motions so that interventions can be prioritized. The tool was also implemented in a GIS environment, in which the worst elements of the investigated road network, requiring on-field refined inspections, are visualized in real-time with a colored scale. With regard to flood actions, the action of river water can apply hydrostatic and hydrodynamic forces to the structural elements of bridges, implying an overloading effect. Nevertheless, the real danger is represented by the combination of the flood (and the velocity of the water) affecting a bridge and the debris (e.g., log) that the flowing water can drag along, colliding with the structural elements. In addition, flowing water could also scour a portion of the soil, characterizing the bridge foundation and reducing the lateral capacity of piles and, therefore, of the entire structure. Anisha et al.[9] proposed a methodology to estimate flood-induced risk for different limit states, providing flood fragility curves. Pregnolato et al.[10] developed a multi-physics modeling approach for assessing the influence of hydrodynamic actions on bridges and the consequent structural response and impact on the road network.

Several studies also aim to combine the above-mentioned risk sources by providing approaches that can be used for improving the study of the structural capacity of existing bridges. For example, Yilmaz et al.[11] investigated the combination of flood and seismic hazards for investigating an existing bridge in California. Similarly, Gehl & D'Ayala[12] developed a multi-hazard risk assessment procedure based on Bayesian network models to account for flood and seismic actions on bridge networks. Mantakas et al.[13] analyzed the seismic response of a case-study bridge in Greece, which was affected by ground movement induced by an active landslide. They performed numerical analyses considering the coupling effect of the seismic-induced motions on stabilization of the soil foundation and the structure, considering the variability of different foundation schemes and stabilization techniques.

Currently, public institutions and transportation managers are working towards the development of procedures for efficient multi-hazard risk assessment and the definition of mitigation strategies. Taking into consideration the Italian case, all the above risk sources are involved in the new risk-mitigation model developed by the Italian Ministry of Transportation[14], released after the well-known collapse of the Polcevera Viaduct[15]. The new Italian guidelines[14] propose a multi-level procedure to be applied to the entire existing bridge stock, which road management companies should adopt for the appropriate management of bridges based on monitoring, maintenance, and retrofit. In this framework, one of the most important phases is represented by the periodical bridge-specific on-site visual inspection, in which expert engineers check the health state of each structural element. This phase covers a key role in the Italian risk-mitigation model, especially for those elements that were scarcely inspected in the past, such as the bearing devices. These latter assume paramount importance in the safety and serviceability of the structure, both from the static (gravity load transfer to substructure) and seismic (transfer of seismic inertia forces to substructure or isolation/dissipation) points of view.

Appropriate schemes of bearing devices, consisting of high-damping elastomeric bearings eventually equipped with lead plugs, can guarantee seismic isolation and dissipation[16]. The seismic response of isolated bridges is characterized by a large vibration period, given by the flexibility of isolators, inducing relevant displacement demand, which is appropriately mitigated by increasing damping provided by the isolation devices. In these structures, the displacement demand is lumped to the isolation systems that are subjected to relevant deformations during the seismic-induced ground motion and can achieve significant deformation-based damage states. Differential displacements of the substructure components subjected to low-moving ground motions induced by active landslides can cause deformation in elastomeric bearings, affecting their capacity during seismic events and increasing the fragility of the bridge.

On this basis, the paper presents a study on the seismic behavior of existing isolated reinforced concrete (RC) bridges subjected to preliminary landslide-induced elastomeric bearing deformation. In particular, a framework is introduced to estimate the influence of landslide-induced bearing deformations on seismic fragility and risk considering several deformation-based damage states. The framework is based on nonlinear time history analyses performed by using scaled natural ground motions and numerical models in which the cyclic behavior of preliminary deformed elastomeric bearings is simulated based on experimental tests available from the scientific literature. The proposed approach was tested on a real-case study, the Santo Stefano viaduct in the Basilicata region (Southern Italy), which was subjected in the past to the abovementioned phenomenon. For the case study, seismic fragility curves were provided, considering and not the observed landslide-induced deformations in elastomeric bearings.

Related Studies

Seismic isolation in RC bridges: the use of elastomeric bearings

When talking about RC bridges, the isolation system is placed on substructure components and acts as a flexible

layer, uncoupling the superstructure from the substructure[17]. The low stiffness of isolation devices induces large values during the vibration period, inducing significant displacement demand under seismic excitation, which is lumped in the isolation layer. In the case of strong seismic actions, the nonlinear response (and hysteretic dissipation) is lumped into the isolation bearings, while the other components (superstructure and substructure) behave elastically. In general, two types of isolation systems can be employed in RC bridges: (1) elastomeric bearings; and (2) sliding bearings[18]. The elastomeric bearings allow the shift of the fundamental frequencies of the structure through a specifically designed horizontal stiffness for the purpose of resonance averting. Instead, the sliding bearings works according to the concept of dissipation through friction, thanks to specific frictional devices that allow seismic isolation. For the purpose of this study, the focus of this section is related to the elastomeric bearings and the seismic behavior of isolated RC bridges equipped by these devices.

The most adopted elastomeric bearings in the practice are the laminated rubber bearings, which are characterized by alternate thin layers of rubber and steel. Low-damping natural rubber bearings (NRB) or high-damping rubber bearings (HDRB) can be used for isolation purposes. Additionally, lead-rubber bearings are characterized by the presence of a central lead core that increases the dissipation capacity. The scientific literature provided several studies over the last 50 years regarding the seismic behavior of bridges with elastomeric bearings, the design of these devices, and the assessment through experimental and numerical analyses. For the purposes of this study, a brief summary of the seismic fragility of isolated bridges is reported. Gardoni & Trejo[19] proposed some probabilistic models to investigate the seismic demand in isolated RC bridges, with the aim of providing a reliability-based approach to bridge design. With this goal in mind, the authors generated a sample of RC NRB-isolated bridges, which were analyzed through sets of ground motion records to derive fragility curves via an approximate formulation. Siqueira et al.[20] investigated the seismic behavior and fragility of isolated RC bridges in Canada retrofitted via NRB. The authors considered the uncertainties related to the mechanical properties of NRBs based on experimental tests in which size and shape factors varied. Dezfuli & Alam[16] investigated the influence of different elastomeric bearing typologies on the seismic fragility of isolated RC bridges. Using NRBs, HRBs, and LRBs on a three-span continuous bridge, the authors assessed the most vulnerable typology despite highlighting the pros of the isolation. Bayat et al.[21] investigated the seismic fragility of skewed RC isolated bridges, accounting for more than 10 types of elastomeric devices, with the aim to define the sub-optimal combination for improving the design of the isolation system. Hassan and Billah[22] investigated the effect of ground motion duration on the seismic response of isolated bridges, equipped with three different types of isolation bearings (among which, LRB). Results suggest that long-duration and high-intensity earthquakes significantly affect the performance of bridges and the isolation system efficiency. Maghsoudi-Barmi et al.[23] investigated the seismic performance of highway isolated bridges equipped with unbonded NRBs. Despite the evident advantages of this system (e.g., easiness and cost of production), properties like bearing connection type, friction coefficient, and aging were considered in the analyses showing possible implications in terms of fragility. Kurino et al.[24] analyzed the seismic fragility of isolated highway bridges, accounting for the rubber deterioration. Results in terms of fragility curves provided an evident lower performance of the isolated bridge when deterioration is accounted, and the necessity of a retrofit solution based on cable restrainers. Wei et al.[17] proposed a study on the seismic fragility of isolated bridges accounting for two aspects: (a) the pier height; (b) the behavior of elastomeric bearings. Firstly, authors performed and experimental campaign comprising different kinds of elastomeric bearings combined with different height piers. From the estimate of the seismic fragility, authors proposed an optimal combination of the above parameters, in a view of new designs. Aghaeidoost and Billah[25] performed a sensitivity analysis on bridge fragility using different modeling approaches for considering the LRBs in isolated RC bridges. Results revealed that hardening effect of elastomer and strength degradation due to the lead core heating assumes a key role.

Influence of preliminary deformation of elastomeric bearings in RC bridges

The seismic behavior of isolated RC bridges is strongly correlated to the performance of bearings devices, which connect substructure with the superstructure. In the case of elastomeric bearings, the design and the assessment of the devices consist in the consideration of axial forces to which they are subjected under gravity loads and the allowable horizontal displacements that they can achieve in the case of seismic excitation. According to the goal to purse through the isolation system, several experimental, analytical, and numerical studies were proposed in the past to investigate the capacity of elastomeric bearings and their behavior under vertical-horizontal actions (e.g., Kikuchi et al.[26], Vemuru et al.[27]). On the other hand, the most recent literature pointed out to consider other factors affecting the nonlinear behavior of elastomeric bearings. With this regard, Mitoulis[28] performed a parametric analysis accounting for uplift effect in elastomeric bearings when horizontal actions invest an isolated bridge. Results showed that a tensile displacement in bearings occurs if the pier is subjected to rotation and emphasized if bearings are placed eccentrically with respect to the pier axis. Very significant are the studies proposed by Moghadam and Konstantinidis[29,30] which investigated with axial loads and horizontal displacements also the top plate rotation of bearings. In the first work, authors proposed a detailed finite element model for elastomeric bearings subjected to top plate rotation and compared the numerical performance with other literature works, while in the second work, authors provided a macro-model for the same purpose. The main results showed that rotation influences the critical shear force of the bearings instead of critical displacement. In addition, a larger vertical stress

can provide a decrease of tangent stiffness. Still, Moghadam & Konstantinidis[31] carried out an experimental campaign in which authors investigated the role of plate rotation in LRB for different axial loads and horizontal displacement. The main result presents a shift up of the hysteresis loop, with a critical force reduction for negative actions (where the term "negative" indicates the opposite direction of the action, assuming a reference system). This problem was recently faced by different authors, which proposed some new mechanical models on the base of Moghadam and Konstantinidis achievements (e.g., Zhang et al.[32], Pishgahi & Taghikhany[33]).

Although several studies are provided for describing the real behavior of isolation systems in bridges under horizontal loads, very few studies face the occurrence of induced deformation in elastomeric bearings, induced for example by landslides. Hence this paper attempts to provide a practical approach for evaluating the variation in terms of seismic fragility of isolated bridges characterized by the above problem. Nevertheless, it is necessary to anticipate that authors do not dispose of any experimental campaigns to accurately evaluate the real performance of the bearings, but this would be a first step in this direction, considering slow and invisible phenomena like landslides can strongly limit the efficiency and the life of such structures.

Influence of Landslide-induced Bearing Deformation on the Seismic Response of Isolated Bridges: Proposal of a Practical Approach

The main aim of this study is to provide a practical methodology to characterize the influence on the seismic performance of bridges isolated by elastomeric bearings when these latter present pre-existing deformations induced by low-moving ground movement. The steps of the proposed procedure are described in the following subsections and briefly summarized in Fig. 1.

Basic knowledge of the bridge

The first step involves a comprehensive knowledge characterization of the bridge under investigation. Being an existing structure (even if built in the recent past), it is necessary to collect data on bridge's geometry and structural features by performing an accurate knowledge process according to the reference code (e.g., see Hendy et al.[34] for Eurocode). The most important aspects to be characterized concern the geometry (e.g., dimensions of each structural element), gravity loads to be considered for seismic analysis and, particularly, information on the nonlinear cyclic response of isolation devices. Considering that the bridge nonlinear response is governed by the isolation system, the mechanical properties of structural materials are of minor importance since superstructure and substructure components are modeled as elastic components (see subSection 3.3). A key information is represented from the original technical documents on elastomeric bearings which are needed to numerically reproduce their response under gravity and seismic loads. Given a sufficient documentation, this step is aimed to determine a numerical (e.g., finite element, FE) model of the investigated bridge without any interference from the surrounding environment. This numerical model (named Model 1—Undeformed) represents the reference one.

Survey and monitoring of landslide-induced deformative phenomena

The second step of the procedure regards the survey and monitoring of the bridge subjected to deformative phenomena. This phase can be performed through several operations, which depend on the available time and economic sources dedicated to the phenomenon identification (this latter can depend also on the importance of the structure within the road network). The operations are subdivided in two categories: (a) short-term survey; (b) long-term monitoring. Regarding to the short-term survey, when the deformation on the structures occurs, expert engineers are involved to carry out an accurate survey of each structural element. Simple methodologies can be employed, such as a full-photographic survey or a plumb line method to detect horizontal deformations of elastomeric bearings. These simple measures allow us to understand at what point the phenomenon is and, above all, what is the current difference with the undeformed configuration, according to the original documentation. In addition, the short-term survey allows establishing the strategy to employ for the long-term monitoring. About the long-term monitoring, several experimental campaigns can be employed, depending on the type of manifested phenomenon. The expression long-term refers to the necessity of carrying out experimental campaigns for a long period, depending on the efficiency of the monitoring system and on the intensity/velocity of the monitored phenomenon. To generalize this step in a view of a landslide action, three types of monitoring campaigns are strongly suggested: (i) a topographic monitoring; (ii) a geotechnical monitoring; (iii) a structural monitoring. The topographic monitoring is useful to accurately define the position of the structural elements for a given acquisition and estimate the displacement trend by repeating acquisitions of the position over time. These measurements should detect displacements and deformations of the substructure components. The measurements can be performed by using the most recent survey techniques (e.g., drones with high-accuracy photogrammetry, laser scanner acquisitions) or by simply using a total station with some collimation points materialized on the structures with reflective devices (e.g., measuring prisms). The campaign should provide periodical measurements, considering a time step of a couple of months, for ensuring appropriate understanding of seasonality effects on the deformation trends. The geotechnical monitoring is essential in problems related to geohazards, and then measurements of slow motions and the evolution of the underground water level are the minimum requirements. In this case, a static monitoring should be employed, by using inclinometers and piezometers. The monitoring time

should be quantified as previously stated for the topographic monitoring. Finally, a structural monitoring is suggested, even if it should be the most expensive among the three above actions and it can provide information about the structural evolution in consequence to base deformations. Accurate monitoring systems (e.g., strain gauges) placed in the right position can suggest the displacement and the velocity of the structural elements motions. Also in this case, the time of the experimental campaign should follow the above suggestions. As output of this step, for purpose of structural and seismic assessments, the following data should be detected: (a) the displacements and the rotations at the base of the piers (and the abutments); the horizontal deformation of the elastomeric bearings and the related rotation of the top steel plate.

Numerical simulations

Once all data are available, two numerical models can be realized, accounting and not for the landslide-induced deformative phenomenon (Model 1-Undeformed and Model 2-Deformed as reported in Fig. 1). For both models, considering the goal to estimate seismic behavior and fragility, simple numerical models can be employed, depending on the analysts' preferences. The modeling strategy is shown in Fig. 2a, where the numerical model should appropriately consider the nonlinear cyclic response of elastomeric bearings, while substructure components and superstructure elastomeric bearings are considered elastic. Particularly, the superstructure can be schematized through a simple frame equipped with an appropriate inertia moments and mass distribution. Three-dimensional models are suggested for analysis in both longitudinal and transverse direction (separately or contemporarily). The elastomeric bearings are characterized by a backbone curve equipped with the proper hysteretic behavior. In the case of LBRs or HDRBs, the backbone is usually elasto-plastic with high hardening while the hysteretic behavior is like-isotropic. If significant, depending on the investigated bridge structural features, the nonlinear behavior of other components should be included in the model[35]. For example, pounding between adjacent decks (for simply supported girder schemes) and between deck and abutments should be modeled by simulating impacts between different elements after gap closure. Similarly, the impacts between superstructure and shear keys in case of large displacements should be represented. If needed, abutment-backfill and soil-structure interactions can be considered.

While the undeformed model does not include the landslide-induced effects, the deformed model should represent the seismic behavior of the bridge under landslide-induced deformed conditions. A schematic and qualitative representation of a landslide-induced displacement scenario resulting in deformation on elastomeric bearings is provided as shown in Fig. 3. In detail, the slow action of low-moving active landslide provokes a roto-translation of the substructure components (a pier is represented in Fig. 2, although the same effect can be recorded for abutments). Given their high flexibility, elastomeric bearings experience deformations since their lower plate is connected to the pier cap, while the upper plate is connected with the superstructure, which behave as an hyperstatic system, counteracting the displacement of the pier. Clearly, bearing deformations are enhanced in continuous-superstructure bridges, while these can be mitigated in simply supported (e.g., isostatic) bridges. The phenomenon can be simply described by a roto-translation of the pier and a different roto-translation of the elastomeric

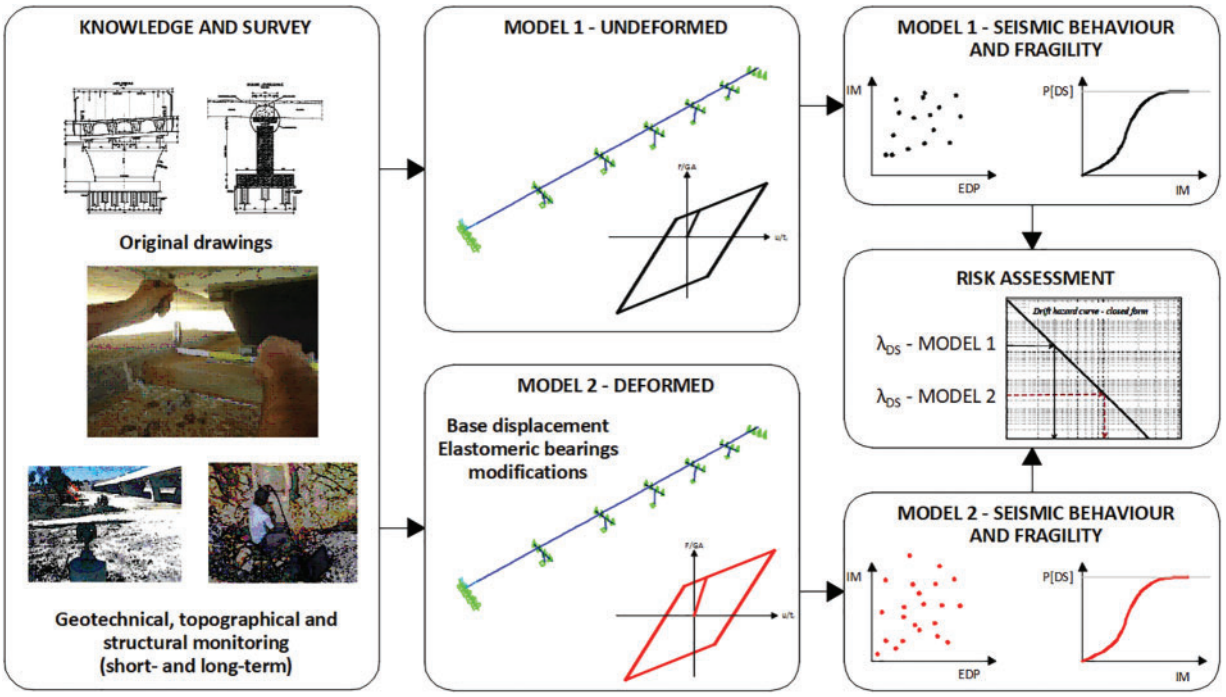

Figure 1. Summary of the proposed approach

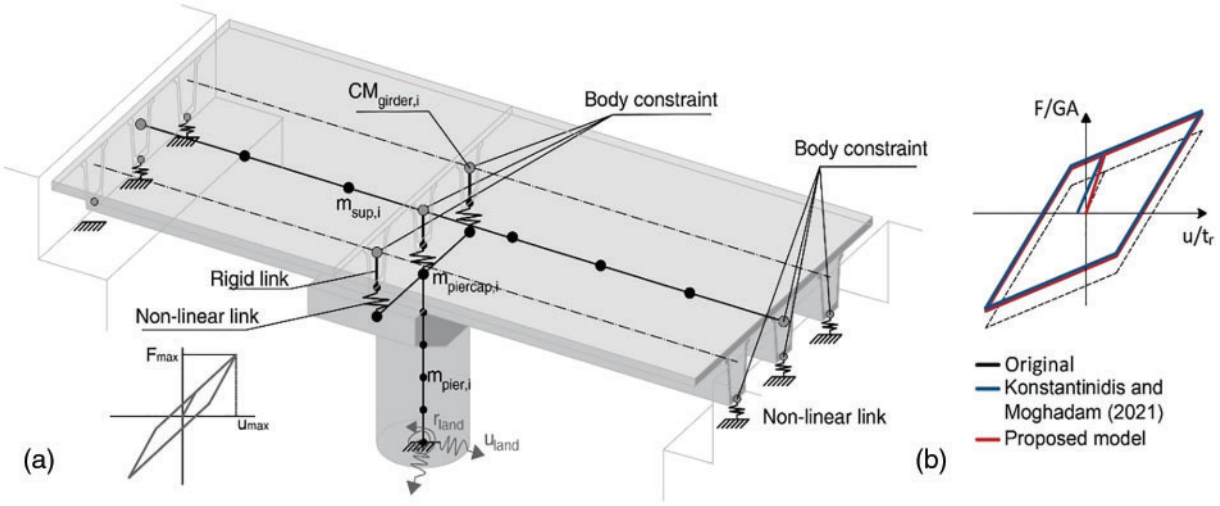

Figure 2. a) Strategy for numerical modeling; b) Proposed modification to elastomeric bearing constitutive law. F/GA represents the ratio between the horizontal force and the elastomer area and shear modulus. u/tr represents the ratio between the horizontal displacement and the rubber thickness

bearings (this latter depends on several factors, such as the transverse and torsional stiffness of the superstructure and their vertical stiffness, which in this study were not considered). To simulate the horizontal displacement, if the output of geotechnical monitoring is available, the model can account for soil-structure interaction and then, soil-structure interaction could be also modeled. On the other hand, if the monitoring is not complete and to benefit the modeling simplicity, it is suggested to simulate the base of the pier like fix and to apply a static displacement pattern with specific values detected in a precise moment, for both analysis directions.

As stated by Moghadam & Konstantinidis[31], preliminary bearing rotation involves modification in the nonlinear response of elastomeric bearings. Given the axial force calculated considering gravity loads, the rotation can be analytically computed after some in-situ measures of each elastomeric bearing. As shown in Fig. 3, right, at the base of the support there is a bottom rotation, θ_B, which is equal to the rotation of the pier if no deformation occurs (it is likely, considering that the landslide action is static, and the pier is subjected to a rigid roto-translation). If the surveyor detects the right and left height of the focused elastomeric bearing (H_1 and H_2 respectively), and the new base in the deformed configuration (L_1), the top rotation, θ_T, can be simply computed as

$$\theta_T = \frac{max\,(H_1, H_2) - min\,(H_1, H_2)}{L_1} \qquad (1)$$

The value of θ_T is relative to the rotated pier and then, it does not depend on the base rotation of the pier.

For sake of completeness, if θ_T should be computed in absolute value, it must be purified by the value of θ_B. Although the estimate is very simple, it provides a likely value of rotation which can be used to shift the elastomeric bearing backbone and the related hysteresis loop of a force computed according to Moghadam & Konstantinidis[31]. The response in terms of hysteresis loop is shown in Fig. 2b, in which the original constitutive law (dashed-black), the abovementioned literature solution (blue) and the simplified proposed ones are shown (red). In detail, in the proposed simplification, the value of the initial stiffness is slightly changed, considering that commercial software does not allow to define a backbone law that does not go through the origin of the axes. It is worth noting that the proposed modification for the backbone of the elastomeric bearings tends to modify only the elastic branch of the real constitutive law, by modifying its stiffness. This numerical trick brings to increase the bearings stiffness, allowing a conservative effect in the achievement of the yielding. Both simplified modeling techniques (displacements at the base of the pier and modified backbone of elastomeric bearings) allows to modify the model according to the observed effect.

Seismic analysis, fragility, and risk quantification

Once numerical models are ready, a probabilistic seismic analysis can be performed to estimate the possible differences on fragility and risk. For this purpose, nonlinear response history analyses (NRHAs) are strongly suggested in literature. For this scope, a record selection is required, which can be performed according to the specific hazard characteristics of the bridge site and the related soil amplification. The record selection should be performed based on the methodology adopted to carry out the probabilistic seismic assessment (e.g., cloud analysis). In this study, a cloud-based fragility analysis[36] by using natural scaled ground-motion records is performed. Regarding to the number of records, being a single-scale analysis, record-to-record variability assumes high significance in the result and then, a high number of records should be desirable. On the other hand, a practical approach as the one proposed cannot require high computational efforts. Hence, the suggestion is to adopt at least 11 records, according to the suggestions provided in ASCE 7-16.[37]

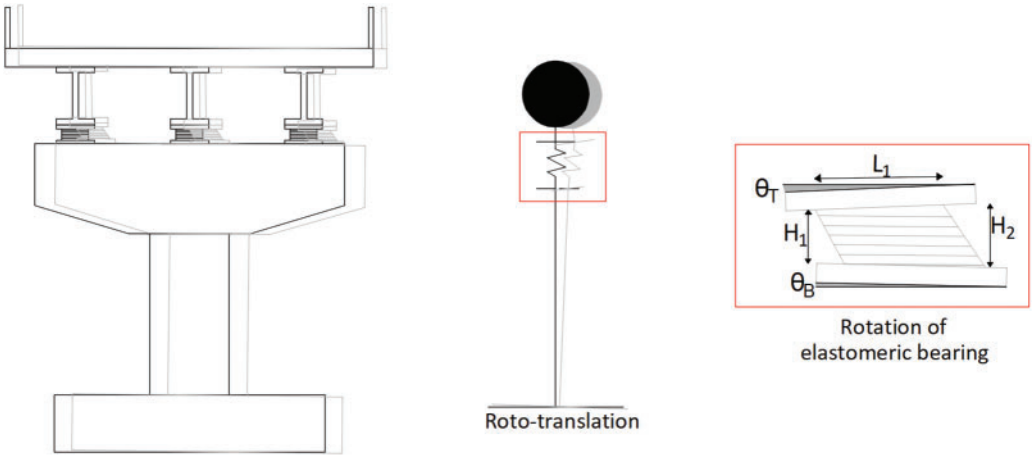

Figure 3. Schematization of landslide effect on a pier with isolation system made through elastomeric bearings

The number of ground motion components depends on the observed displacement. If the displacement occurs in one direction (e.g., transversal), the main effects shall be observed in that direction and monodirectional analysis can be performed, but in general, bi-directional analysis can be employed. The intensity of the record is quantified in terms of and intensity measure, IM, which for the case at hand can be set in terms of peak ground acceleration, PGA, or spectral acceleration of the first vibration period, $Sa(T_1)$ (for more information, see O'Reilly[38]). After running analysis, the results can be recorded in terms of engineering demand parameter, EDP, which for the case of isolated RC bridge can be selected as the shear strain of elastomeric bearings (γ), according to Aghaeidoost & Billah[25]. Given the distribution of EDP|IM, fragility curves can be quantified, by referring to different damage states or different limit states. For the case at hand, the suggestion is to refer to the damage states (DS) as a percentage of γ values, according to Zhang & Huo[39]. It is worth specifying that for a row of elastomeric bearings on the same pier of pier cap, the DS can be considered exceeded when the first support exceeds the predefined limit. Eq. (2) shows the generic analytical form used in this study for a given fragility relationship, expressing the probability of violating, given a DS, $P(DS|IM)$. The fragility model is expressed by the normal cumulative distribution function, $\phi(\cdot)$, based on the probabilistic seismic demand model represented by a power-law model ($EDP = aIM^b$) which is fitted to the "cloud data" in the $\log IM - \log EDP$ plane. The parameters a and b are estimated through regression analysis resorting to the least square method. This logarithmic standard deviation (or dispersion, $\beta_{EDP|IM}$) is quantified via Eq. (3), where N is the number of ground motions gm.

$$P(DS|IM) = \phi\left(\frac{\ln EDP_{DS} - \ln aIM^b}{\beta_{EDP|IM}}\right) \tag{2}$$

$$\beta_{EDP|IM} = \sqrt{\frac{\sum_{gm=1}^{N}\left(\ln EDP_{gm} - \ln aIM_{gm}\right)^2}{N-2}} \tag{3}$$

Given the fragility curve for each DS and for both numerical models, risk can be quantified. The risk is quantified as the mean annual frequency of exceeding the damage state λ_{DS}. For this last step, the simplified formulation of the risk can be employed[40]:

$$\lambda_{DS} = \lambda_{IM,50}^{DS} e^{\left(\frac{1}{2}k_{DS}^2\beta_{EDP|IM}^2\right)} \tag{4}$$

where $\lambda_{IM,50}^{DS}$ is the mean annual frequency of exceeding of the median IM causing a DS (associated to 50% probability of exceedance) and k_{DS} is the slope of the hazard curve for the median IM causing the DS. From the quantification of the risk for both model configurations (undeformed and deformed), monetary losses could be estimated in the case of earthquake occurrence for each specific performance. This quantification can easily support the transportation managers in near-future decisions, where a strong increment of λ_{DS} from the undeformed case to the deformed case implies a timely structural and geotechnical intervention, while a limited reduction could lengthen the time.

Case-Study Application of the Proposed Procedure: Santo Stefano Viaduct

Description of the S. Stefano Viaduct and landslide-induced deformations

The "Santo Stefano" Viaduct is placed on the Bradanica road, which links the municipalities of Matera and Candela, between the regions Basilicata and Puglia, Southern Italy. The bridge was built in 2013 to overpass the Santo Stefano canal. It extends for about 180 m with six spans. A graphic description of the case-study bridge is reported in Fig. 4. The continuous superstructure is composed of four precast U-shaped girders with height of 1.80 m, covered by an RC slab having a thickness equal to 0.25 m. The piers are founded on large-diameter bored piles. Two abutments, consisting of RC walls, were built to support the access embankments to the viaduct. The piers present height ranging from 5.70 and 8.90 m. As shown in Fig. 4c, three wall-type piers exhibit a like-trapezoidal shape with variable cross-section dimensions along the height, while the two highest piers are characterized by framed structure. The girders are connected to the piers through a line of elastomeric bearings placed on

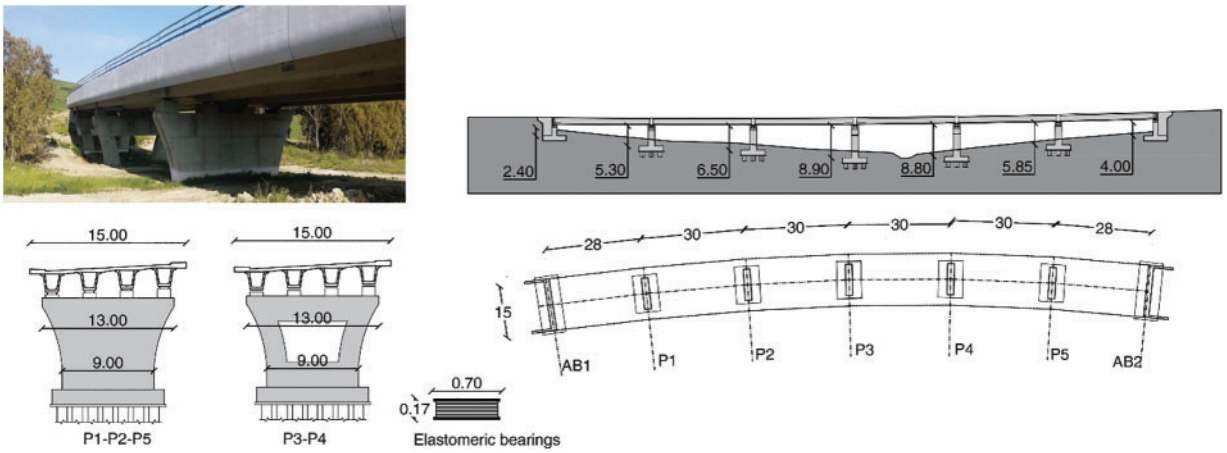

Figure 4. Description of the case-study bridge (photo, planimetric view, longitudinal view)

Table 1. Characteristics of the elastomeric bearings

Effective stiffness (k_h) [kN/mm]	Vertical stiffness (k_v) [kN/mm]	Elastomer diameter [mm]	Elastomer thickness [mm]	Total height [mm]	Side total length [mm]	Displacement capacity Δ_{max} [m]	Shear modulus (G) at $\gamma = 1$ [MPa]
3.08	2617	700	100	237	750	0.2	0.8

baggies. Four bearings are placed on each pier and designed to present an equivalent viscous damping equal to about 12%. Properties assigned to elastomeric bearings are listed in Table 1. In the end, it is worth noting that the bridge presents a slight curvature along its longitudinal extension, with a radius of about 700 m. In Fig. 4, a photo of the bridge, a planimetric view and a longitudinal view are reported.

On the basis of the preliminary in-situ observations, two specific monitoring campaigns were performed to identify the real causes of the bridge motion: (a) a geotechnical monitoring; (b) a topographic monitoring. The geotechnical monitoring was characterized by a combination of piezometers and inclinometers in the points of greater deformation (abutment in Candela direction), in order to highlight deep sliding surfaces. The results showed a sliding surface at 14 m below ground level, with an observed displacement of 2.5 cm in 3 months, which provokes the failure of some inclinometers. Piezometric measurements showed, in Candela direction, a piezometric level of about $1 \div 2$ m depth from the surface while, on the Matera side, it was close to ground level.

The topographic monitoring was elaborated by a precise measurement campaign aimed to identify all displacements with a millimetric accuracy. It was characterized by several measures made each three months and by using a total station and some measuring prisms placed on the structural elements of the bridge. The results show the evolution of the phenomenon, which was identified with a motion of the piers and abutments in the impluvium direction. From the global phenomenon point of view, the entire bridge was moving in the direction of the curvature radius center caused by the landslide, and each pier was subjected to a rigid motion. In the subsequent years, others monitoring campaigns were proposed to better characterize the phenomenon. Herein, of interest is not to define all experimental campaigns, but the definition of the mitigation actions to limit the landslide. To this scope, three drainage wells were inserted to intercept groundwater and lower neutral pressures in foundation soils and, thus, limit movements. In addition, a structural health monitoring system was permanently placed on the structure, with the aim to monitor all the effects that the observed phenomenon has on the bridge over the time.

In conclusion, from the structural point of view, some interventions were carried out: (a) controlled demolition of the abutment back-walls in the contact areas with the beams and reconstruction of the back-walls to restore the original gap size; (b) replacement of deformed bearing devices (lifting of the superstructure, removal of the deformed elastomeric bearings as shown in Fig. 5 and positioning of new ones).

Numerical modeling

Although the deformed elastomeric bearings were replaced and appropriate mitigation interventions were carried out to prevent further damages, the aim of this study is to assess the sensitivity of the seismic fragility of the bridge affected by landslide-induced deformation. In other words, the goal is to evaluate the seismic risk and damage probability referring to the evaluation and monitoring time period in which the elastomeric bearings presented a preliminary deformation. To this scope, the framework defined in Section 3 was employed. It is worth noting that this approach should be adopted in cases similar to the analyzed one to evaluate variation in seismic fragility and risk considering long time periods ranging from the observation of the phenomenon to the execution of interventions. Additionally, the variation in

Figure 5. Permanent deformation observed on the HDRBs, after one year from the bridge construction

seismic risk measured by the presented methodology should be adopted as a decision support for transport authority's operators which are in charge for defining if interventions are needed or not.

First, the numerical model of the bridge was created without considering any elastomeric bearing deformations (referred to as Model 1-Undeformed hereafter). In this study, the numerical model was built in SAP2000 software[41], although any software package suitable for bridge modeling can be adopted. The modeling strategy shown in Fig. 2 was used. In detail, all piers were modeled as frame elements fixed at the base, while abutments were simulated as fixed supports on which elastomeric bearings are leaned. The deck was simulated as a single frame element connected to the piers through a set of two-node links simulating the elastomeric bearings. As anticipated in sub-Section 3.3, this assumption strongly reduces modeling efforts in seismic analysis where the superstructure is considered to respond elastically and to simulate a realistic seismic mass distribution along the bridge length. To the frame simulating the superstructure, distributed loads were addressed, accounting for the seismic combination[42] of the structural and non-structural loads. These loads were considered according to the original drawings. Despite the bridge presents a slight curvature ratio along its longitudinal direction, the simplification of straight trend was assumed to penalize the response in transverse direction under horizontal actions (no longitudinal action components were considered). The nonlinear response of elastomeric bearings was simulated by using multilinear-plastic links, in which the backbone was defined according to Table 2, while the hysteresis loop was defined considering a kinematic hysteretic behavior.

The second model (hereafter referred to as Model 2-deformed) reflects the features of Model 1, while introducing some modifications accounting for landslide-induced effects. First, the displacements measured by means of the topographic monitoring system were assigned to the base node of substructure components in transverse direction. Additionally, the backbone response assigned to the elastomeric bearings were modified considering the effect of rotation of the upper plate, according to the approach proposed by Moghadam and Konstantinidis[29]. All the values of the landslide-induced base displacements and bearing-specific nonlinear parameters, in terms of yielding and ultimate force (F_y and F_u, respectively) and displacement (Δ_y and Δ_u) are reported in Table 2. The sign + or – indicates for the forces, the positive and negative values in the backbone.

Given the numerical models, eigenvalue analyses were performed. The first period of vibration for Model 1 and Model 2 is equal to 1.60 s. Therefore, a record selection was performed as follows. First, a target spectrum for the site of interest is extracted considering an expected PGA equal to 0.40 g. A dataset of ten scaled natural records is first extracted by using the tool REXEL proposed by Iervolino et al.[43]. Spectrum-compatibility was checked with respect to the target spectrum and by using the Eurocode 8 provisions that suggest to select records in order to have differences between mean and target spectra of +30% and −10% for a range of periods of interest. The period of interest is fixed between 1.00 and 2.50 s considering that high-frequency modes are of minor importance for the analyzed case study. Subsequently, this record dataset is further scaled for achieving a PGA of the target spectrum equal to 0.30 and 0.20 g. In this way, a total of 30 ground-motion records is obtained. In Fig. 6a, elastic (5% damping) acceleration spectra of the selected set of ground motion records, mean and target spectra are reported. Additionally, to perform the risk assessment, the hazard curve (Fig. 6b) for the site of interest is extracted by using the tool REASSESS by Chioccarelli et al.[44].

Fragility analysis and risk assessment

On this base, 30 runs of NRHA were performed on both numerical models. For the sake of simplicity, given the illustrative purpose of this study, only the seismic response in transverse direction was considered. For both models, a post-processing check was performed after NRHAs to avert the occurrence of nonlinear mechanisms in the structural elements (i.e., in the piers). EDP were extracted in terms of shear strain γ demand of the elastomeric bearings. To interpret the achieved results and for describing how NRHA results were elaborated to obtain bearing shear strains γ, the outcomes for a randomly selected record (in terms of displacement registered for significant nodes) are shown in Figs. 7a and 7b. The initial displacement (initial condition for NRHA) of the bearing top node is indicated as continuous dark-grey curve. Clearly, this is equal to 0 for model 1, while it reflects the initial landslide-induced deck deformed

Table 2. Modeling parameters of elastomeric bearings and landslide-induced base displacement, indicated for each vertical element and model

Model	Component	Base displacement (m)	F_y[kN]	F_u [kN]	Δ_y [m]	Δ_u [m]
Model 1	All	–	40	627	0.004	0.20
Model 2	Ab1	0.10	40	−541/+713	0.004	0.20
	P1	0.12	40	−563/+691	0.004	0.20
	P2	0.07	40	−585/+669	0.004	0.20
	P3	0.03	40	−538/+716	0.004	0.20
	P4	0.06	40	−573/+781	0.004	0.20
	P5	0.07	40	−517/+737	0.004	0.20
	Ab1	0.07	40	−494/+760	0.004	0.20

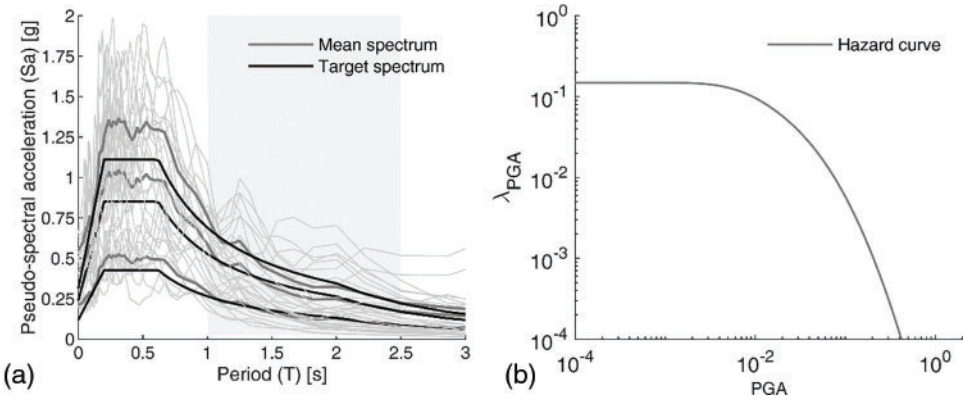

Figure 6. a) Acceleration spectra for the selected set of records, mean and target spectra; b) Hazard curve

shape for model 2. The maximum displacement demand registered for bearing top nodes during NRHA (in positive and negative direction) is also presented via dashed light-grey curves. The position of the lower bearing node is additionally indicated by means of black circular markers. Note that no significant displacements of the lower bearing node (i.e., pier top node) are observed during the seismic excitations. Fig. 7c reports the shear strain demand calculated for the two models. The comparison between Figs. 7a and 7b shows the significant influence of the landslide-induced effects in the NRHA-based displacement profile. For model 1, the displacement demand for bearing devices reflects a "parabolic" distribution. This is also reflected on γ values for model 1 reported in Fig. 7c. The maximum demand was registered for the bearing device placed on the central pier (i.e., indicated as P3). Similar results were observed for the other NRHAs. For model 2, the initial displacement pattern of bearing top nodes reflects the hyperstatic response of the superstructure under landslide-induced differential pier displacements (black markers). Therefore, the bearings were subject to an initial shear strain demand before the NRHA was conducted. The displacement demand induced by NLRHA exhibited an irregular shape with respect to the former case. For each bearing device, the shear strain demand was computed considering the differential displacement between the top and the bottom nodes. As shown in Fig. 7c, this resulted in a general increase in shear strain demand with respect to model 1 for the bearing devices. Also, in this case, the highest γ was related to the central pier.

The maximum γ registered among the bearing devices was extracted for each NRHA and used as EDP for fragility analysis. The peak ground acceleration (PGA) was considered as IM. To compute fragility curves, the continuous relationship between IM and EDP was estimated by employing the power law approximation, as suggested by Cornell et al.[45]. Four damage states (DS) were considered, associated with slight, moderate, extensive, and complete damage conditions, as suggested by Zhang and Huo[38]. DS thresholds are indicated in Table 2. Note that although elastomeric bearings may experience shear strain values up to 400%, the DS4 was associated with a limit shear strain equal to 250% in order to avoid large deck displacements and deck unseating[25].

Accounting for all the above-mentioned DSs, fragility curves for the bridges in Model 1 and Model 2 are reported in the graphs in Fig. 8. As expected, landslide-induced deformations on elastomeric bearing induced a general increase in fragility for all the considered DSs. Observing the fragility curves, the most significant fragility variation was registered to DS1 (Fig. 8a), where the median value of the fragility curve (probability equal to 50% of exceeding a given DS) presented an increase equal to 44.7%. Conversely, the influence of permanent landslide-induced deformations on elastomeric bearings decreased for increasing DS limits.

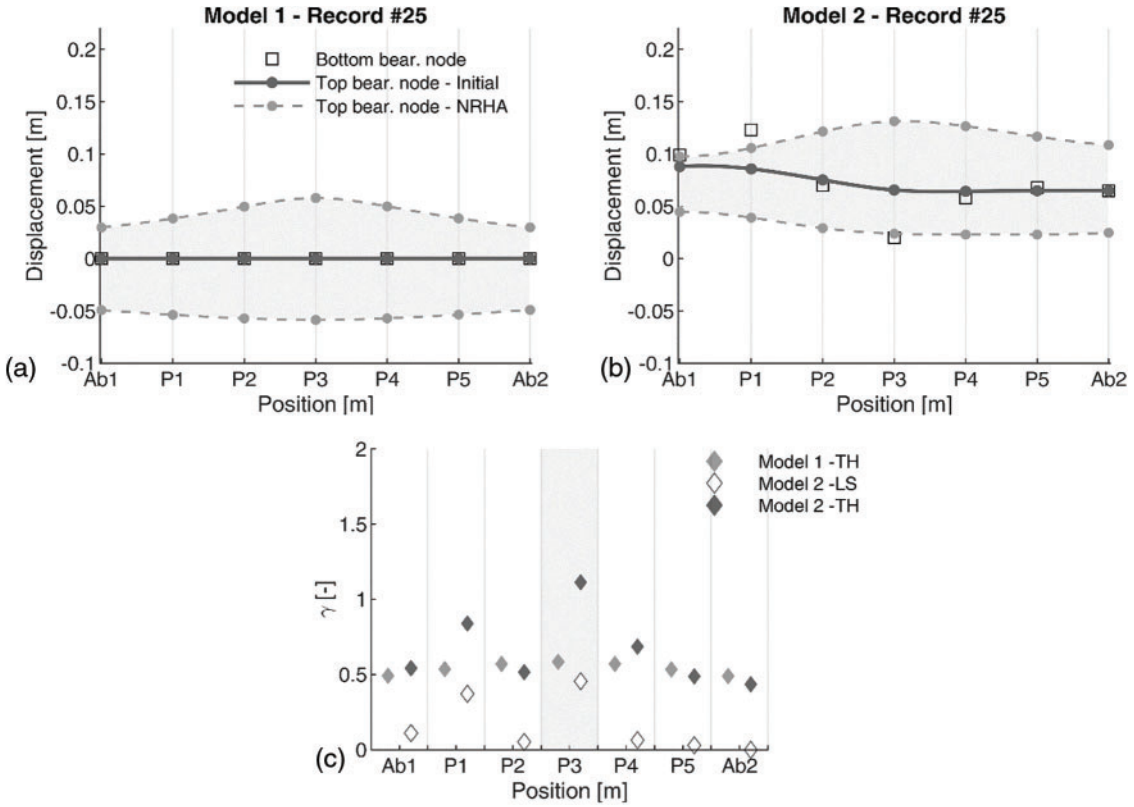

Figure 7. Displacement demand calculated for a randomly selected record (a) Model 1 and (b) Model 2 and shear strain demand (c)

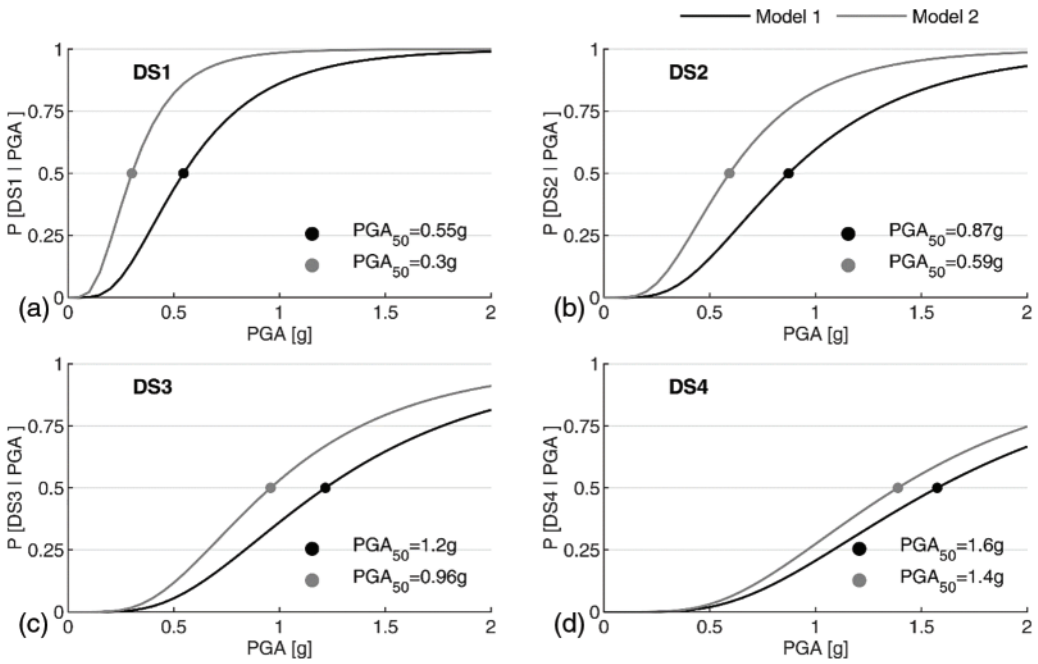

Figure 8. Fragility curves of Model 1 (Undeformed) and Model 2 (Deformed), accounting for damage states DS1, DS2, DS3, DS4

Indeed, the variation in median fragility curves between Model 1 and Model 2 decreased to 32.0%, 21.2%, and 11.8% for DS2, DS3, and DS4, respectively. For all the DS, a similar fragility dispersion was computed, equal to 0.5 and 0.55 for Model 1 and Model 2. As expected, the obtained results suggest that the initial landslide-induced phenomenon on the elastomeric bearings assumes a more important effect on the lower DSs (e.g., DS1 and DS2) than the higher

Table 3. Damage state thresholds in terms of shear strain γ

Demand parameter	DS1	DS2	DS3	DS4
γ_{DS} (%)	100%	150%	200%	250%

Table 4. λ_{DS} values for MODEL 1 and MODEL 2, accounting for damage states DS1, DS2, DS3, and DS4

$\lambda_{DS}\left[10^{-3}\right]$	DS1	DS2	DS3	DS4
Model 1–Undeformed	0.1863	0.0429	0.0134	0.0050
Model 2–Deformed	0.8955	0.1406	0.0298	0.0076

DSs (e.g., DS3 and DS4). This is because the value of the initial displacement, expressed in terms of γ, represents a higher contribute with reference to the threshold values (see Table 3) for the lower DSs than the one observed with reference to the threshold values for the higher DSs.

Finally, from the probabilistic measure of the damage, the risk was quantified by means of the λ_{DS} values. Results for Model 1 and Model 2 and for all the considered damage states are reported in Table 4. As expected, the values of λ_{DS} were significantly higher for Model 2 than Model 1. The highest increase was observed for DS1, where λ_{DS} reaches $0.89 * 10^{-3}$ for Model 2, with respect to $0.18 * 10^{-3}$ for Model 1. Conversely, a slight increase was observed for DS4 where λ_{DS} values are comparable. Clearly, these outcomes in terms of risk are significantly correlated to the adopted hazard curve reflecting the hazard condition of the bridge location.

Conclusions and Further Developments

The study concerns seismic fragility and risk of reinforced concrete (RC) bridges isolated via elastomeric bearing devices subjected to differential displacements induced by slow-moving landslides. The paper describes a practical approach to investigate the seismic fragility and risk of RC bridges isolated via elastomeric bearings, which experience preliminary deformations induced by the landslide-induced effects involving the bridge. The proposed methodology was based on numerical modeling to represent the structure in undeformed and deformed conditions and adopts nonlinear response history analyses to generate fragility curves according to the cloud-based approach. Using two numerical models, it is possible to quantify the influence of landslide-induced effects on seismic fragility and risk and to provide decision-support indications to transport authorities in charge of ensuring the safety of bridges.

The proposed approach was tested on a real-life case study, the *Santo Stefano* viaduct in Italy, which was subjected in the past to elastomeric bearing deformation given by an active landslide phenomenon. The application proved that for the case at hand, the landslide-induced effects had a strong influence on the seismic fragility, particularly referring to the low-damage state. This effect was weakened for more severe damage states. Clearly, the results achieved are strictly related to the case study analyzed. However, the presented methodology can be adopted by means of typological approaches and parametric analysis to estimate the influence on fragility and risk by varying the intensity of landslide-induced differential displacements. Additionally, further developments of the methodology may consider introducing other components in the numerical model, such as shear keys and pounding effects, which can be significant for two-directional seismic analysis.

Acknowledgements

The authors acknowledge the Italian Consortium FABRE for the financial support.

References

[1] Gidaris I, Padgett JE, Barbosa AR, et al. Multiple-hazard fragility and restoration models of highway bridges for regional risk and resilience assessment in the United States: state-of-the-art review. *J Struct Eng*. 2017;143(3):04016188.

[2] Borzi B, Ceresa P, Franchin P, et al. Seismic vulnerability of the Italian roadway bridge stock. *Earthq Spectr*. 2015;31(4):2137–2161.

[3] Abarca A, Monteiro R, O'Reilly GJ. Exposure knowledge impact on regional seismic risk assessment of bridge portfolios. *Bull Earthq Eng*. 2022;20(13):7137–7159.

[4] Cademartori M, Sullivan TJ, Osmani S. Displacement-based assessment of typical Italian RC bridges. *Bull Earthq Eng*. 2020;18:4299–4329.

[5] Gentile R, Nettis A, Raffaele D. Effectiveness of the displacement-based seismic performance assessment for continuous RC bridges and proposed extensions. *Eng Struct*. 2020;221(2):110910.

[6] Nettis A, Iacovazzo P, Raffaele D, et al. Displacement-based seismic performance assessment of multi-span steel truss bridges. *Eng Struct*. 2022;254(2):113832.

[7] Peduto D, Elia F, Montuori R. Probabilistic analysis of settlement-induced damage to bridges in the city of Amsterdam (The Netherlands). *Transp Geotech*. 2018;14:169–182.

[8] Nettis A, Massimi V, Nutricato R, et al. Satellite based interferometry for monitoring structural deformations of bridge portfolios. *Autom Constr*. 2023;147:104707.

[9] Anisha A, Jacob A, Davis R, et al. Fragility functions for highway RC bridge under various flood scenarios. *Eng Struct*. 2022;260:114244.

[10] Pregnolato M, Winter AO, Mascarenas D, et al. Assessing flooding impact to riverine bridges: an integrated analysis. *Nat Hazards Earth Syst Sci*. 2022;22(5):1559–1576.

[11] Yilmaz T, Banerjee S, Johnson PA. Uncertainty in risk of highway bridges assessed for integrated seismic and flood hazards. *Struct Infrastruct Eng*. 2018;14(9):1182–1196.

[12] Gehl P, D'Ayala D. System loss assessment of bridge networks accounting for multi-hazard interactions. *Struct Infrastruct Eng*. 2018;14(10):1355–1371.

[13] Mantakas A, Tsatsis A, Loli M, et al. Seismic response of a motorway bridge founded in an active landslide:

a case study. *Bull Earthq Eng*. 2023;21:605–632. doi:10.1007/s10518-022-01544-3.
[14] Ministero delle infrastrutture (MIT). Linee guida per la classificazione e gestione del rischio, la valutazione della sicurezza ed il monitoraggio dei ponti esistenti. 2020 (in Italian).
[15] Calvi GM, Moratti M, O'Reilly GJ, et al. Once upon a time in Italy: the tale of the morandi bridge. *Struct Eng Int*. 2022;29:198–217. doi:10.1080/10168664.2018.1558033.
[16] Dezfuli F, Alam MS. Effect of different steel-reinforced elastomeric isolators on the seismic fragility of a highway bridge. *Struct Control Health Monitor*. 2017;24(2):e1866.
[17] Wei W, Yuan Y, Igarashi A, et al. Experimental investigation and seismic fragility analysis of isolated highway bridges considering the coupled effects of pier height and elastomeric bearings. *Eng Struct*. 2021;233(7):111926.
[18] Kunde MC, Jangid RS. Seismic behavior of isolated bridges: a-state-of-the-art review. *Electron J Struct Eng*. 2003;3:140–170.
[19] Gardoni P, Trejo D. Probabilistic seismic demand models and fragility estimates for reinforced concrete bridges with base isolation. *Earthq Struct*. 2013;4(5):527–555.
[20] Siqueira GH, Sanda AS, Paultre P, et al. Fragility curves for isolated bridges in eastern Canada using experimental results. *Eng Struct*. 2014;74:311–324.
[21] Bayat M, Daneshjoo F, Nistico N, et al. Seismic evaluation of isolated skewed bridges using fragility function methodology. *Comput Concrete*. 2017;20(4):419–427.
[22] Hassan AL, Billah AM. Influence of ground motion duration and isolation bearings on the seismic response of base-isolated bridges. *Eng Struct*. 2022;222(2):111129.
[23] Maghsoudi-Barmi A, Khansefid A, Khaloo A, et al. Probabilistic seismic performance assessment of optimally designed highway bridge isolated by ordinary unbonded elastomeric bearings. *Eng Struct*. 2021;247(3):113058.
[24] Kurino S, Wei W, Igarashi A. Seismic fragility and uncertainty mitigation of cable restrainer retrofit for isolated highway bridges incorporated with deteriorated elastomeric bearings. *Eng Struct*. 2021;237(3):112190.
[25] Aghaeidoost V, Billah AM. Sensitivity of seismic fragility of base-isolated bridges to lead rubber bearing modeling technique. *Struct Control Health Monit*. 2022;e2971.
[26] Kikuchi M, Nakamura T, Aiken ID. Three-dimensional analysis for square seismic isolation bearings under large shear deformations and high axial loads. *Earthq Eng Struct Dyn*. 2010;39(13):1513–1531.
[27] Vemuru VS, Nagarajaiah S, Mosqueda G. Coupled horizontal–vertical stability of bearings under dynamic loading. *Earthq Eng Struct Dyn*. 2016;45(6):913–934.
[28] Mitoulis SA. Uplift of elastomeric bearings in isolated bridges subjected to longitudinal seismic excitations. *Struct Infrast Eng*. 2015;11(12):1600–1615. doi:10.1080/15732479.2014.983527.
[29] Moghadam SR, Konstantinidis D. Finite element study of the effect of support rotation on the horizontal behavior of elastomeric bearings. *Compos Struct*. 2017a;163:474–490.
[30] Moghadam, SR, Konstantinidis D. Simple mechanical models for the horizontal behavior of elastomeric bearings including the effect of support rotation. *Eng Struct*. 2017b;150:996–1012.
[31] Moghadam SR, Konstantinidis D. Experimental and analytical studies on the horizontal behavior of elastomeric bearings under support rotation. *J Struct Eng*. 2021;147(4):04021024.
[32] Zhang Z, Yang L, Xiang S, et al. New macroscopic model for predicting the horizontal behavior of elastomeric bearings under end-plate rotation. *Structures*. 2023;47(1):1086–1093.
[33] Pishgahi F, Taghikhany T. Mechanical model for seismic nonlinear behavior of rubber bearings with end-rotation in highway bridges. *Structures*. 2023;47(4):875–890.
[34] Hendy CR, Sandberg J, Shetty NK. Recommendations for assessment Eurocodes for bridges. In: *Proceedings of the Institution of Civil Engineers-Bridge Engineering*; 2011; Thomas Telford Ltd, pp. 3–14.
[35] Nielson BG, DesRoches R. Seismic fragility methodology for highway bridges using a component level approach. *Earthq Eng Struct Dyn*. 2007;36(6):823–839.
[36] Jalayer F, Ebrahimian H, Miano A, et al. Analytical fragility assessment using unscaled ground motion records. *Earthq Eng Struct Dyn*. 2017;46(15):2639–2663.
[37] ASCE 7–16. *Minimum Design Loads for Buildings and Other Structures: Commentary*. American Society of Civil Engineers; 2017. doi:10.1061/9780784412916.
[38] O'Reilly GJ. Seismic intensity measures for risk assessment of bridges. *Bull Earthq Eng*. 2021;19(9):3671–3699. doi:10.1007/s10518-021-01114-z.
[39] Zhang J, Huo Y. Evaluating effectiveness and optimum design of isolation devices for highway bridges using the fragility function method. *Eng Struct*. 2009;31(8):1648–1660.
[40] Jalayer F, Cornell CA. A technical framework for probability-based demand and capacity factor (DCFD) seismic formats. 2002. https://peer.berkeley.edu/sites/default/files/0308_f._jalayer_c._allin_cornell.pdf.
[41] CSI. *SAP2000 v.24, Advanced Structural Analysis Program–Manual*. Berkeley: Computer and Structures Inc.; 2022.
[42] DM 17/01/2018. *Aggiornamento delle Norme Tecniche per le Costruzioni*. Gazzetta Ufficiale n. 42. February 20. Rome; 2018 (in Italian).
[43] Iervolino I, Galasso C, Cosenza E. REXEL: Computer aided record selection for code-based seismic structural analysis. *Bull Earthq Eng*. 2010;8:339–362. doi:10.1007/s10518-009-9146-1.
[44] Chioccarelli E, Cito P, Iervolino I, et al. REASSESS V2.0: software for single- and multi-site probabilistic seismic hazard analysis. *Bull Earthq Eng*. 2019;17:1769–1793. doi:10.1007/s10518-018-00531-x.
[45] Cornell CA, Jalayer F, Hamburger RO, et al. Probabilistic basis for 2000 SAC federal emergency management agency steel moment frame guidelines. *J Struct Eng*. 2002;128(4):526–533.